Enhancing Color Image Compression with Linear Polynomial Coding and Adaptive Inter-Prediction

Marwa B. Al-Obaidi[1], Ghadah Al-Khafaji[1], Dr. Mohammed M. Siddeq[2]

[1] *Department of Computers, College of Science, Baghdad University, Baghdad, Iraq.*

[2] *Department of Computer Engineering, Technical College/Kirkuk, Northern Technical University, Iraq*

***Abstract*— This paper introduces a proposed technique for compressing color images with the objective of minimizing their size. The technique divides the image into three bands: a source band representing the Green channel, and a non-source band representing the Red and Blue channels. The source band is encoded using a lossless 2D_linear polynomial technique, which ensures that the compressed image retains its original quality. The non-source bands employ an adaptive inter-prediction technique to enhance the efficiency of compression. The experimental results provide evidence supporting the effectiveness of the proposed technique, surpassing traditional compression methods and even outperforming the widely used JPEG technique. Moreover, the technique maintains optimal image quality while achieving efficient compression. The proposed technique achieves a reduction in image size of approximately 13.8 KB and a compression ratio (CR) of about 14, surpassing the capabilities of JPEG. Overall, the proposed technique offers a promising approach to color image compression, providing a means to reduce the size of color images while preserving their quality.**

***Keywords*— Compression of color images, linear polynomial encoding, and color inter -prediction based compression.**

1. Introduction

color image compression lies as an efficient elegant way for archiving and transmission of color images in modern systems, which unfortunately suffer from the huge size of bytes consumptions that lead to utilized standard available techniques such as JPEG, PNG, and BMP with constraints of using since most of them of the lossy base along the inability to use regions independently and inherited problems of redundancy(s) types exploited [1-4]. Generally image compression techniques classified according to the way of redundancy(s) exploited, here the color images overburden with spectral, spatial, coding and psychovisual, if the first three exploited, namely of statistical one the lossless base adopted, while if the psychovisual exploited either alone or combined with statistical redundancy the lossy base adopted, each one have advantages/disadvantages, the utilization of one over the other determined by problem nature **[5-7].**The lossless techniques appropriate for color images, since to preserving image quality identically, but with low compression performances, that leads to utilized the lossy standard techniques in spite of degreases quality to gain more compression performance, with constraints of unnoticeable degradation [8-13]. Color images exhibit high spectral redundancy between the RGB color bands. Early approaches to color compression focused on compressing each band separately without considering the correlation between them, resulting in limited compression performance. Subsequent research explored color transformation models to effectively exploit the spectral redundancy, but still relied on the same marginal approach [13-17].

Today, inter-base prediction techniques offer a solution to the color image compression problem by treating it similarly to video compression. These techniques identify the source band based on its correlation or importance and remove certain bands, replacing them with predicted bands derived from the source. Inter-prediction is a crucial technique employed in video and image compression to enhance compression efficiency. It entails predicting pixel values within a frame using neighbouring pixels or previously encoded frames. By capitalizing on the temporal or spatial redundancies inherent in video and image data, inter-prediction significantly reduces the volume of data that must be encoded and transmitted such as [18-20].

Polynomial coding is an advanced technique for spatial image compression that aims to efficiently eliminate the spatial redundancy present within an image. This technique utilizes mathematical models to accurately represent non-overlapping blocks of the image using a small set of coefficients that result in low error or residual that basically classified either into linearity or non-linearity, along 1D/2D block nature, several attempted aimed to improve the techniques performances The underlying concept of polynomial coding involves the effective modeling of image partitions to achieve optimal compression results such as [21-27].

In this paper, the main objective is to examine and suggest effective approaches for compressing color images. The specific emphasis is placed on exploring different inter-prediction modeling techniques as potential means of achieving

DOI:http://doi.org/10.24086/cocos2024/paper.1524

efficient compression. The paper aims to contribute to the field by proposing novel methods that can enhance the compression performance for color images.

2. Adaptive Inter-Prediction Base Techniques

The proposed color image compression mixture between linear polynomial coding and inter-prediction schemes of RGB base to exploits the spectral redundancy(s) effectively, that discussed using the following steps below, and the process illustrated in **Figure.1** is followed to compress the color image:

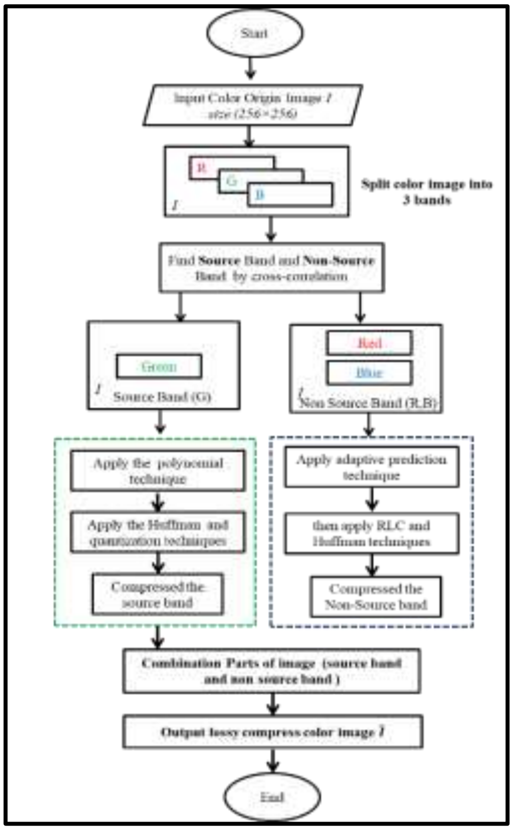

Figure 1. Flowchart of the proposed system of Adaptive inter prediction color base.

Step 1: Utilize the original uncompressed color image I of size N×N×3.

Step 2: The image I is split into its bands (I_R, I_G, I_B), where each band corresponds to the R, G, and B image channels and has a size of N×N. These bands contain high spectral redundancy.

$$\left.\begin{array}{l} I_R = I(:\,;\,:\,;1) \\ I_G = I(:\,;\,:\,;2) \\ I_B = I(:\,;\,:\,;3) \end{array}\right\} \quad (1)$$

Step 3: Choose the source color band, according to the cross-correlation measure that adopted by [6],

$$R_{(xband,yband)} = \frac{\sum_{x=0}^{n-1}\sum_{y=0}^{n-1} C_{(xband,yband)}}{\sqrt{\sum_{x=0}^{n-1}\sum_{y=0}^{n-1} C_{(xband,yband)} C_{(xband,yband)}}} \quad (2)$$

Step 4: For Source band: Apply lossless linear polynomial coding to ensure error-free reconstruction that composed of the sub-steps bellow:

1. Loading the input uncompressed source band I_G, which is in BMP format and has a size of N×N**.**
2. Partitioning the image I_G into non-overlapping blocks of a fixed size, such as 4×4 or 8×8. The coefficients are then computed using equations (3-5)

$$a_0 = \frac{1}{n \times n}\sum_{i=0}^{n-1}\sum_{j=0}^{n-1} I(i,j) \quad (3)$$

$$a_1 = \frac{\sum_{i=0}^{n-1}\sum_{j=0}^{n-1} I(i,j)\times(j-x_c)}{\sum_{i=0}^{n-1}\sum_{j=0}^{n-1}(j-x_c)^2} \quad (4)$$

$$a_2 = \frac{\sum_{i=0}^{n-1}\sum_{j=0}^{n-1} I(i,j)\times(j-y_c)}{\sum_{i=0}^{n-1}\sum_{j=0}^{n-1}(j-y_c)^2} \quad (5)$$

The coefficient a0 represents the mean (average) of a block of size n×n in the original image I. The coefficients a1 and a2 capture the ratio of the pixel sum multiplied by the squared distance from the center in the i and j coordinates **[18]** respectively.

$$x_c = y_c \frac{n-1}{2} \quad (6)$$

The terms (j-x_c) and (i-y_c) measure the distance of the pixel coordinates to the center of the block (x_c, y_c). [**18]**

3. Apply uniform scalar quantization/Dequantization of the computed polynomial coefficients, where each coefficient is quantized using different quantization step.

$$a_0Q = round\left(\frac{a_0}{QS_{a0}}\right) \rightarrow a_0D = a_0Q \times QS_{a0} \quad (7)$$

$$a_1Q = round\left(\frac{a_1}{QS_{a1}}\right) \rightarrow a_1D = a_1Q \times QS_{a1} \quad (8)$$

$$a_2Q = round\left(\frac{a_2}{QS_{a2}}\right) \rightarrow a_2D = a_2Q \times QS_{a2} \quad (9)$$

Where the polynomial coefficients a_0Q, a_1Q, and a_2Q are quantized using specific quantization steps QS_{a0}, QS_{a1}, and QS_{a2}. The dequantized polynomial coefficients are denoted as a_0D, a_1D, and a_2D.

4. Calculate the predicted image ($\tilde{I}$) value by using the dequantized polynomial coefficients for each encoded block representation.

$$\tilde{I} = a_0D + a_1D(j - X_c) + a_2D(i - y_c) \quad (10)$$

5. Compute the residual (Res) or prediction error by taking the difference between the original image (I) and the predicted image $\tilde{I}$.

$$Res(i,j) = I(i-j) + \tilde{I}(i-j) \quad (11)$$

6. Perform scalar uniform quantization and dequantization of the residual part, following the same procedure as described in Step 3.

$$ResQ = round\left(\frac{Res}{QS_{Res}}\right) \rightarrow ResD = ResQ \times QS_{Res} \quad (12)$$

7. Apply symbol coding techniques to eliminate the coding redundancy present between the quantized values of the residual and the polynomial coefficients.
8. To reconstruct the compressed image, the decoder adds the estimated image to the dequantized residual.

$$\hat{I}(i,j) = \tilde{I}(i-j) + ResD(i-j) \quad (13)$$

Step 5: For Non-Source bands: The inter-prediction based technique is applied using two models that utilize the reference band and a seed value from the current band (non-reference) to estimate the current band**. Figure.2** illustrates these two models.

First Model

$$\tilde{X} = \frac{W + (X_r - W_r) + N + (X_r - N_r) + P + (Xr - Pr)}{3} \quad (14)$$

Second Model

$$\tilde{X} = \frac{W + (X_r - W_r) + N + (X_r - N_r) + P + (Pr - Xr)}{2} \quad (15)$$

The current pixel value X is estimated by a predictor $\tilde{X}$, which relies on neighboring intensity values from both the current band (P, N, W, and X) and a reference band (Pr, Nr, Wr, and Xr).

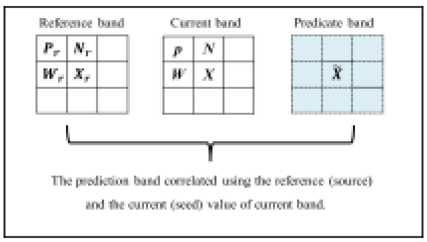

Figure 2. Adaptive inter prediction color base**.**

Step 6: Calculate the residuals for the non-source bands by taking the difference between the original band and the predicted band (as shown in equation 16). Then, perform uniform quantization and Dequantization of the residuals using a scalar uniform approach (as shown in equation 17).

$$Res(i,j) = Referance_{band}(i-j) - Prediction\ of\ Referance_{band}(i-j) \quad (16)$$

$$Res\ (i,j) = round\left(\frac{Res}{Qs_{Res}}\right) \rightarrow ResD = ResQ \times QS_{Res} \quad (17)$$

The quantized residual image (ResQ) is obtained by applying quantization to the residual image, using the quantization step (QS_{Res}). The dequantized residual image (ResD) is obtained by reversing the quantization process on the quantized residual image.

Step 7: The compressed information of the inter-prediction technique, including the reference band, is encoded and decoded using Huffman coding techniques.

Step 8: To reconstruct the decoded compressed image, each band is rebuilt separately using the predicted image. Then, the reconstructed bands are added together to form the final compressed or decoded image.

3. EXPERIMENTAL RESULTS

To evaluate the performance of the proposed system, three standard color square images of size 256×256 pixels were used for testing see **Figure.3**. The images were divided into blocks of size 4×4, and lossless linear polynomial coding with quantization coefficients of 1, 2, and 2 was applied. The quantization residual levels (QRes) ranged from 10 to 50.
The compression ratio was calculated by dividing the size of the original image by the size of the compressed image in bytes. Additionally, the Peak Signal-to-Noise Ratio (PSNR) between the original image I and the decoded image was used as a

Test images	Original Image	Red channel	Green channel	Blue channel
Lena				
Girl				
Vegetable				

Figure 4. Band for standard test images in RGB base was separated.

DOI:http://doi.org/10.24086/cocos2024/paper.1524

measure of fidelity or degradation. The PSNR was computed using equations (18).

$$PSNR(I,\hat{I}) = 10log_{10}\frac{(255)^2}{\frac{1}{N\times N}\sum_{i=0}^{n-1}\sum_{j=0}^{n-1}\left[\hat{I}(x-y)-I(x-y)\right]^2} \quad (18)$$

Figure 3. The three Tested Images of Size 256×256, color images: (a) Lena, (b) girl (c) Vegetable.

The presented T**able.1** illustrates that the cross-correlation values were highest when comparing the green band with the red and blue bands. This signifies a significant correlation between the green band and the other color bands within the RGB system. Consequently, the green band was chosen as the source band for the inter-prediction technique in the tested images. The selection of the appropriate source band is crucial for achieving precise predictions and efficient compression in the RGB system.

Table 1. The cross correlation between color bands and the selection the source band in RGB system.

Test images	**Cross_ Correlation (R,G)**	**Cross_ Correlation (R,B)**	**Cross_ Correlation (B,G)**	**Source band**	**Non source bands**
Lena	0.8895	0.7089	0.9222	G	B,R
Girl	20.771	0.6819	0.9126	G	B,R
Vegetable	0.6522	0.0325	0.2732	G	B,R

From the three **Tables 2 to 4** above, upon analyzing these tables, the following observations can be made:

• Image Sizes: The sizes of the compressed images vary depending on the model used. The second and third models generally achieve smaller sizes, indicating better compression efficiency.

Table 2. The Size in byte of the tested images by using the models with Q.step for residuals =10

Tested images	first_model	**second_model**
Lena	16109	12965
girl	22961	14793
vegetable	21353	15970

Table 3. The CR of the test image by using the models with Q.step for residuals =10

Tested images	first_model	**second_model**
Lena	12.2049	15.1645
girl	8.5627	14.2480
vegetable	9.2075	12.3111

Table 4. The PSNR of the test image by using the models with Q.step for residuals=10

Test images	first_model	**second_model**
Lena	32.5881	37.5732
girl	37.8188	37.6353
vegetable	38.6161	37.6161

Compression Ratio: The compression ratio can be calculated by dividing the original image size by the compressed image size. Smaller sizes indicate higher compression ratios. The second and third models tend to achieve higher compression ratios due to their smaller sizes.

• PSNR Values: The PSNR values reflect the quality of the compressed images compared to the original images. Higher PSNR values indicate better quality and less distortion. The first and fourth models generally achieve higher PSNR values, suggesting better image quality.

• Trade-off: There is a trade-off between image size and image quality. Models that achieve smaller sizes may sacrifice some image quality, while models with higher image quality may result in larger file sizes. The second models offer a better

DOI:http://doi.org/10.24086/cocos2024/paper.1524

balance, because the compression ratio is the best while maintaining good image quality ratios. These results were based on the quantization step = 10 for the residual coefficients.

Table 5. The comparison between the best model and traditional method with quantization step 1,2,2, for coefficients and Q.step=10 for residuals

Test image	**Best model (second)**		Traditional model	
	CR	**PSNR**	CR	PSNR
Lena	**15.1645**	**37.5732**	5.5913	38.4025
girl	**14.2480**	**37.6353**	5.2367	38.0798
vegetable	**12.3111**	**37.6161**	5.3975	39.0772

From **Table.5 ,**For Lena, the Best Model achieves a CR of 15.1645 and a PSNR of 37.5732, while the Traditional Model has a lower CR of 5.5913 and a slightly higher PSNR of 38.4025. Similar trends can be observed for the girl and vegetable images, where the Best Model consistently shows higher CR and competitive PSNR values compared to the Traditional Model .Overall, the Best Model demonstrates superior performance in terms of compression ratio and image quality, highlighting the effectiveness of the proposed approach in color image compression as shown in **Figure.5.**

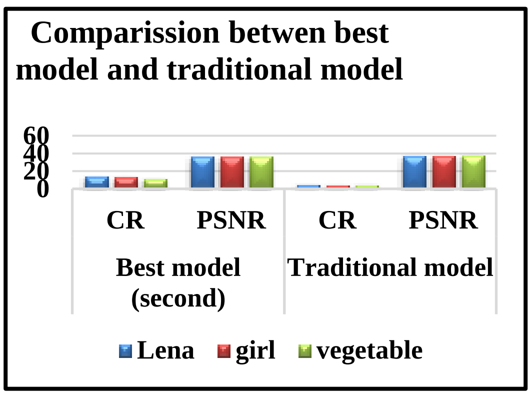

Figure 5 . Comparison of measure CR and PSNR between the third model (best model) and the traditional model.

Test image	**Best model (second)**		Jpeg	
	CR	**PSNR**	CR	PSNR
Lena	**15.1645**	**37.5732**	8.0672	36.5382
girl	**14.2480**	**37.6353**	9.2308	33.0791
vegetable	**12.3111**	**37.6161**	8.4581	34.7141
total	**14**	**37.6**	8.6	34.78

Overall, when considering the total average performance from **Table 6**, the Best Model demonstrates a CR of 14 and a PSNR of 37.6, while the JPEG method has a CR of 8.6 and a PSNR of 34.78. These results indicate that the Best Model achieves better compression efficiency and maintains higher image quality compared to the JPEG method as shown in **Figure.6**.

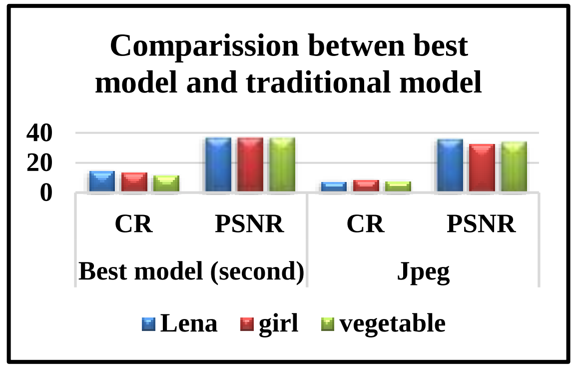

Figure 6. Comparison of measure CR and PSNR between the third model (best model) and the stranded technique JPEG.

4. CONCLUSIONS

The presented Best Mode (second model) for color image compression, which incorporates adaptive inter-prediction and quantization techniques, demonstrates superior performance compared to the conventional JPEG method. The Best Model achieves higher compression ratios while preserving image quality, as evidenced by the higher peak signal-to-noise ratio (PSNR) values. These results validate the effectiveness of the proposed approach for efficient and high-quality compression of color images. The Best Model is ability to adaptively predict and quantize image data showcases its potential for improving compression efficiency and maintaining visual fidelity in various applications that require color image compression. The results highlight the advantages of the presented Best Model, which combines inter-prediction modeling, quantization, and adaptive techniques, offering efficient and effective solutions for color image compression.

REFERENCES

1. Qasim, A.J., Din, R. and Alyousuf, F.Q.A. Review on techniques and file formats of image compression. *Bulletin of Electrical Engineering and Informatics* **2020**, 9(2), 602-610. Doi:10.11591/eei.v9i2.2085.
2. Kumar, S.N., Bharadwaj, M.V. and Subbarayappa, S., 2021, April. Performance Comparison of Jpeg, Jpeg XT, Jpeg LS, Jpeg 2000, Jpeg XR, HEVC, EVC and VVC for Images. In 6th International Conference for Convergence in Technology (I2CT), **2021** 1-8. IEEE.Doi: 10.1109/I2CT51068.2021.9418160.
3. Williams, D.M. Performance Overhead of Lossless Data Compression and Decompression Algorithms: A Qualitative Fundamental Research Study. Doctoral dissertation, Northcentral University. 2022
4. Kaya, Ş.M. and Akçay, M.A.,. Image compression performance comparison of RLE and LZV algorithms for effective big data management: A case study. *Anadolu Bil Meslek Yüksekokulu Dergisi* **2023,** 17(66), 149-160.Doi:10.17932/IAU.ABMYOD.2006.005/abmyod_v17i66004.
5. Rahman, M.A. and Hamada, M. *Lossless image compression techniques: A state-of-the-art survey. Symmetry* **2019**, *11*(10), 1274. Doi:10.3390/sym11101274.
6. Otair, M., Abualigah, L. and Qawaqzeh, M.K. Improved near-lossless technique using the Huffman coding for enhancing the quality of image compression. *Multimedia Tools and Applications* **2022**, *81*(20), 28509-28529. Doi:10.1007/s11042-022-12846-8.
7. Zerva, M.C., Christou, V., Giannakeas, N., Tzallas, A.T. and Kondi, L.P. An improved medical image compression method based on wavelet difference reduction. *IEEE Access* **2023,** *11, 18026*-18037. Doi:10.1109/ACCESS.2023.3246948.
8. Messaoudi, A., Benchabane, F. and Srairi, K. DCT-based color image compression algorithm using adaptive block scanning. *Signal, Image and*

Video Processing **2019**, *13*(7), 1441-1449. Doi: 10.1007/s11760-019-01492-7.

9. Salih, Y.A., Mohammed, A.A. and George, L.E. Improved image compression scheme using hybrid encoding algorithm. *Kurdistan Journal of Applied Research* **2019**, *4*(2), 90-101. Doi:10.24017/science.2019.2.9.
10. Sultan, B.A. and George, L.E. Color image compression based on spatial and magnitude signal decomposition. *International Journal of Electrical and Computer Engineering (IJECE)* **2021**, *11*(5), 4069-4081. Doi:10.11591/ijece.v11i5.pp4069-4081.
11. Abdulelah, A.A., Hamed, S.H.A., Rasheed, M., Shihab, S., Rashid, T. and Alkhazraji, M.T.K. The Application of Color Image Compression Based on Discrete Wavelet Transform. *Journal of Al-Qadisiyah for computer science and mathematics* **2021**, *13*(1), 18. Doi:10.29304/jqcm.2021.13.1.762.
12. Elakkiya, S. and Thivya, K.S. Comprehensive review on lossy and lossless compression techniques. *Journal of the Institution of Engineers (India): Series B* **2021**, 1-10. Doi: 10.1007/s40031-021-00686-3.
13. Hussein, N.H. and Ali, M.A. Medical Image Compression and Encryption Using Adaptive Arithmetic Coding, Quantization Technique and RSA in DWT Domain. *Iraqi Journal of Science* **2022**, 2279-2296. Doi:10.1016/j.neucom.2020.04.138.
14. Meyer, A., Genser, N. and Kaup, A. Multispectral image compression based on HEVC using pel-recursive inter-band prediction. In 2020 IEEE 22nd International Workshop on Multimedia Signal Processing (MMSP) *2020*, September, 1-6. IEEE. Doi:10.1109/MMSP48831.2020.9287132.
15. Su, W.H. Advanced machine learning in point spectroscopy, RGB-and hyperspectral-imaging for automatic discriminations of crops and weeds: A review. *Smart Cities* **2020**, *3*(3), 767-792. Doi: 10.3390/smartcities3030039.
16. Liu, X., An, P., Chen, Y. and Huang, X . An improved lossless image compression algorithm based on Huffman coding. *Multimedia Tools and Applications* **2022**, 81(4), 4781-4795. Doi: 10.1007/s11042-021-11017-5.
17. Kuzio, O. and Farnand, S. Comparing practical spectral imaging methods for cultural heritage studio photography. *ACM Journal on Computing and Cultural Heritage* **2022**, 16(1), 1-13. Doi: 10.1145/3531019.
18. Al-Khafaji, G. and Bassim, M. Color image compression of inter-prediction base. *International Journal of Computer Science and Mobile Computing* **2019**, *8*(11), 65-70.
19. Al-Khafaji, G. and Al-Kazaz, H.B . Adaptive color image compression of hybrid coding and inter-differentiation based techniques. *Int J Comput Sci Mobile Compu* **2019*t***, *8*(11), 65-70.
20. Galiano, D.R., Del Barrio, A.A., Botella, G. and Cuesta, D. Securing high-resolution train videos encoded with HEVC and inter prediction mode. *Computers in Industry* **2020**, *121*, 103258. Doi:10.1016/j.compind.2020.103258.
21. Al-Khafaji, G. Linear Polynomial Coding with Midtread Adaptive Quantizer. *Iraqi Journal of Science* **2018**, *59*(1c), 585-590. Doi:10.24996/ijs.2018.59.1C.15.
22. AL-Hadithy, S.S. Adaptive 1-d polynomial coding of c621 base for image compression. *Turkish Journal of Computer and Mathematics Education (TURCOMAT)* **2021**, *12*(13). 5720-5731.
23. Al-Khafaji, G. and George, L.E. Grey-Level image compression using 1-d polynomial and hybrid encoding technique. *Journal of Engineering Science and Technology* **2021**, *16*(6), 4707-4728. Doi: 10.5829/ije.2023.36.02b.05.
24. Ahmed, Z.J., George, L.E. and Hadi, R.A. Image Signal Decomposition Using Polynomial Representation with Hybrid Lossy and Non-Lossy Coding Scheme. *Iraqi Journal of Science* **2022**, 4559-4575. Doi:10.24996/ijs.2022.63.10.38.
25. Mahdi, N.S. and Ghadah, A.K. Image Compression using Polynomial Coding Techniques: A review. *Journal of Al-Qadisiyah for computer science and mathematics* **2022**, *14*(2), 70 Doi: 10.29304/jqcm.2022.14.2.968.
26. AL-Khafaji, G.K., Rasheed, M.H., Siddeq, M. and Rodrigues, M. Adaptive Polynomial Coding of Multi-base Hybrid Compression. *International Journal of Engineering, Transactions B: Applications* **2023**, *36*(2), 236-252. Doi:10.5829/IJE.2023.36.02B.05.
27. Nandyal, S. and Gogi, H.K.,. Comparative Analysis of Intra-and Inter-Prediction Compression Techniques for Endoscopic Videos. In *ICT Analysis and Applications: Proceedings of ICT4SD 2022*, 533-541. Singapore: Springer Nature Singapore. Doi:10.1007/978-981-19-5224-1_54.